ELSEVIER

Journal of Power Sources 52 (1994) 55–59

JOURNAL OF POWER SOURCES

Carbon fibres and natural graphite as negative electrodes for lithium ion-type batteries

R. Yazami, K. Zaghib, M. Deschamps

Laboratoire d'Ionique et d'Electrochimie du Solide de Grenoble (URA CNRS 1213), ENSEEG, BP 75, 38402 Saint-Martin-d'Hères Cedex, France

Received 27 January 1994; in revised form 22 April 1994; accepted 23 April 1994

Abstract

Carbon fibres (CFs), from different origins, and natural graphite are used as host lattices for lithium electrochemical intercalation and de-intercalation in organic liquid and solid polymer electrolytes, respectively. In both systems, irreversible behaviour occurred during the first cycle of which the origin is tentatively discussed. The reversible capacity of the mesophase CFs-based electrodes, which is related to the total relative amount of lithium exchanged with the electrolyte during the charge/discharge operations, is found to increase with their crystallinity. Some thermodynamic data associated with the formation of the stage-1 graphite–lithium compound in polymer electrolyte-based cells are determined.

Keywords Lithium-ion batteries, Carbon fibres, Polymer electrolytes; Carbon–lithium

1. Introduction

Carbon–lithium compounds Li_xC_6 ($0 \leqslant x \leqslant 1$) are used in mass production as a reversible negative electrode in the so-called 'lithium-ion' battery [1]. During the battery charge/discharge operations, lithium is intercalated and de-intercalated into/from the carbon host without any solvent co-intercalation following the scheme:

$$6C + xLi^+ + xe^- \longrightarrow Li_xC_6 \quad (1)$$

When the stage-1 binary compound LiC_6 is formed at the end of the charge operation, the electrode relative volume expansion is around 10% (d_{002} varies from 3.35 to 3.71 Å). The host lattice experiences small deformation, therefore the number of intercalation/de-intercalation cycles may reach up to 1200 cycles [2]. In addition to the high cycleability which also strongly depends on the nature of the electrolyte, the carbon–lithium electrode increases the safety of the lithium battery (no dendritic growth) and has a low working potential in the 0 to 0.75 V versus Li^+/Li range. Moreover, the theoretical specific capacity stored during the formation of LiC_6 from carbon is 372 mAh/g.

Among the various carbon materials which have been evaluated for their potential use as reversible carbon–lithium electrodes (CFs) were extensively studied in the few last years [3–9]. In addition to their relative ease of handling and shaping in composite electrodes, CFs constitute a good family of carbon materials to investigate the conjugated effects of the carbon precursor and the heat treatment temperature (HTT) on the electrode performance. CFs deriving from organic polymers such as PAN (poly(acrylonitrile)) have a low ability for graphitization, therefore their reversible specific capacity is low [5]. Those derived from petroleum or coal pitches mesophase (MCFs) show an increasing crystal ordering with HTT which enhances their lithium storage capability. Reversible capacity values of $C = 220$ mAh/g and $C = 180$ mAh/g were reported with a radially oriented MCFs [9] and with MCFs treated at 2800 °C [7], respectively. Vapour grown CFs (VGCFs) show a reciprocal behaviour compared with MCFs since the C value decreased with the HTT, the highest reported value being 282 mAh/g for a VGCF treated at 1100 °C [6].

Other important parameters are known to affect the carbon electrode capacity such as the nature of the electrode composition [10] and the electrolyte [11]. Ideally, the electron and the ion distribution within the electrode should be as efficient and as homogeneous as possible. The use of an elastomere and ionic conductor such as poly(ethylene oxide) (PEO) as binder of the composite electrode was shown to confer good mechanical and electric (ionic) properties [12]. Acetylene black (AB) can be also added to the electrode in order

SSDI 0378-7753(94)01933-M

to improve the electrode conductance, but in doing so one decreases the faradaic yield, η_{F_1}, of the first discharge/charge cycle as a consequence of the large irreversible capacity of AB [13].

In this work, we have used several CFs in a composite electrode with PEO and AB in a liquid electrolyte. The capacity loss expressed by η_{F_1} which is the ratio of de-intercalated to intercalated lithium amounts during the first cycle and the reversible capacity will be evaluated and discussed in relation with the CFs crystal properties and the graphite/PEO interfacial properties.

2. Experimental

2.1. Carbonaceous materials

Three types of carbonaceous materials were used in this study: CFs, natural, and pyrolytic graphite. The CFs are produced from three kinds of precursors: an isotropic pitch from Union Carbide/Amoco (UCC-2, UCC-32), a mesophase pitch from Tonen (FT 500 and FT 700), and PAN-based fibre from Toray (T 300). CFs were heat-treated under air at 350 °C during 20 min to remove the protective (sizing) polymer thin film; then they were ground in a mortar to reduce their length to a 0.5 to 1 mm powder.

Natural graphite flakes from Madagascar were ground and passed through a sieve of 200 mesh and used in polymer electrolyte cells. Highly oriented pyrolytic graphite from Union Carbide was used for the thermodynamic measurements after chemical lithiation.

Prior to their use, the carbon powders were evacuated under vacuum at 300 °C for 10 h to remove the moisture. The golden colour highly oriented pyrolytic graphite-based LiC_6 was used after its synthesis in POE electrolyte cells.

2.2. Composite electrode and electrochemical cells

For the tests carried out in liquid electrolyte (1 M solution of $LiBF_4$ in a propylene carbonate:ethylene carbonate:dimethoxyethane (1 vol:1 vol:2 vol), pallets with a diameter of 13 mm were prepared, by mixing the CF powder (55 wt.%) with a preparation containing AB (22 wt.%), PEO (11 wt.%) and fine powder of poly(ethylene) (PE) (12 wt.%), dispersed in acetonitrile. After the evaporation of the excess of acetonitrile at room temperature, the mixture is pressed under 2 t/cm^2 to form a pellet. The pellets (of about 30 mg total weight) were dried under vacuum at 180 °C for 10 h, then put into RC2430-type button cells.

In the polymer electrolyte-based cells, the composite electrode was obtained from a suspension in acetonitrile of a mixture containing graphite (70 wt.%) and $P(EO)_8LiClO_4$ (30 wt.%). The suspension is then spread over a stainless-steel disc of 16 mm diameter. The acetonitrile is evaporated at 60 °C in air and then under vacuum at room temperature for few hours. The average total weight of the dried electrode is 7 mg.

Blank tests have been carried out with only AB in order to determine its relative contribution to the composite electrode specific capacity. This contribution was found less than 5% in cells using either electrolytes.

The electrochemical tests were carried out at room temperature in the liquid electrolyte and at 81 °C (±1 °C) in the polymer electrolyte. Galvanostatic cycling was performed with such current values that the formation of LiC_6 in Eq. (1) occurs theoretically in 20 h (*C*/20 rate). The potential ranges of (10 mV to 1.2 V) for liquid electrolyte and (5 mV to 1.5 V) in the polymer electrolyte ($P(EO)_8LiClO_4$) were used. Slow scanning voltammetry (1 mV/min) and thermal potentiometry in the 70 to 120 °C range were applied to the Li/PEO–$LiClO_4$/LiC_6 cells.

3. Results and discussion

3.1. Crystal characterization

X-ray diffraction analysis was performed to determine the carbon interlayer spacing (d_{002}) and the coherence length in the *c*-direction, L_c. Table 1 gives these data for the different CFs. As expected, L_c increases when d_{002} becomes closer to 3.35 Å, characteristic of the highly crystallized graphite.

3.2. Galvanostatic cycling

3.2.1. Liquid electrolyte

Figs. 1 and 2 show the first and tenth intercalation/de-intercalation cycles obtained with the CFs: FT 500, UCC-2, FT 700, UCC-32 and T 300. Typically, during the first cycle, the discharge curve lasts longer than the charge curve which means that more lithium has been transferred to the carbon than has been removed from it. The faradaic yield, η_{F_1}, which is given by the ratio of removed lithium:transferred lithium is roughly between 80 and 90%. This ratio increases after the

Table 1
Origin and crystal characteristics of the carbon fibres used in this study

Origin	Precursor	Code	d_{002} (Å)	L_c (Å)
Toray	PAN	T 300	3.42	71
Union Carbide	Isotropic pitch	UCC-2	3.40	102
Tonen	Pitch mesophase	FT 700	3.37	158
Tonen	Pitch mesophase	FT 500	3.40	107
Union Carbide	Isotropic pitch	UCC-32	3.365	228

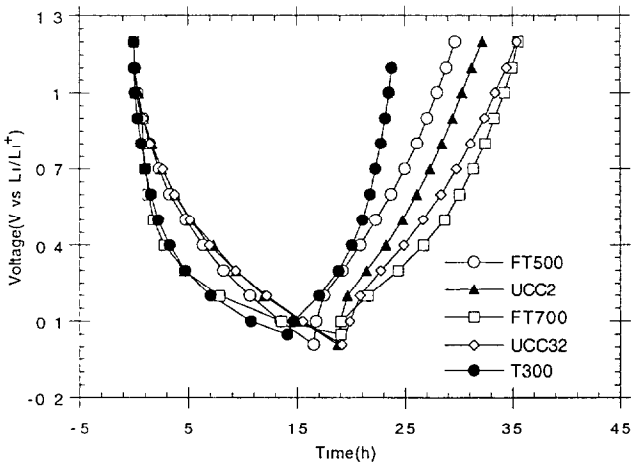

Fig. 1. First cycle (C/20): discharge/charge curves of a Li/PC, EC, DME, $LiBF_4$/carbon fibre cell.

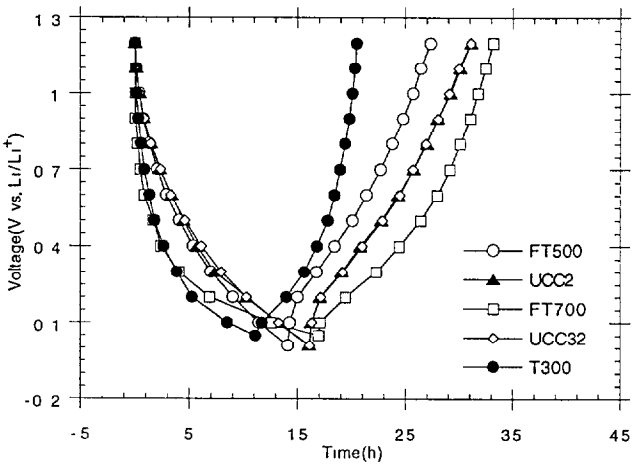

Fig. 2. Tenth cycle at (C/20): discharge/charge curves of a Li/PC, EC, DME, $LiBF_4$/carbon fibre cell.

first cycle and then stabilizes as shown in Table 2. Other characteristic data are presented in Table 2, such as e_0 = initial potential of the cell, $D_{1(10)}$ = specific capacity during the first (10th) discharge, $C_{1(10)}$ = specific capacity during the first (10th) charge, and faradaic yields of the corresponding cycles, $\eta_{F1(10)}$. All data are average values of at least three reproducible measurements.

The CFs-based electrodes have been classified in a decreasing C_{10} values order, C_{10} designs the reversible capacity of the electrode since the C_n (n = cycle number) do not vary very significantly after the first cycle even though the faradaic yield of each cycle is relatively low ($\leqslant 94\%$) indicating that some lithium is still lost at each cycle. We have taken into account the reversible capacity of the added AB [13] in C_{10} values given in Table 2.

For CFs, the C_{10} values tend to increase with the graphitization degree. FT 700 fibres, treated at a higher temperature, have a reversible capacity 22% higher than that obtained with FT 500. A weaker increase is obtained with UCC-2 and UCC-32 fibres after HTT (about 6.5%). Our results are in agreement with those reported by the Iijima et al. [7] who used home-made MCFs. On the contrary, VGCFs have a decreasing reversible capacity with the graphitization heat treatment [6]. These differences in behaviour may result from the nature of the active sites where reduced lithium is stored in MFCs and VGCFs. Since lithium can be either plated on the surface (including the micropores if any) and/or intercalated between the graphene layers, both the active surface area and the crystallinity, which are affected by the HTT, should control the reversible capacities of the respective CFs.

The origin of the low faradaic yield during the first cycle is generally attributed to the following effects:

(i) formation of a protective film on the surface of the fibres; this film results from the decomposition of the electrolyte which involves an irreversible lithium consumption [14–16];

(ii) deposition of metallic lithium, especially at low potential close to 0 V versus Li^+/Li, and

(iii) formation of a residual carbon–lithium compound from which lithium cannot be removed in the experiment time scale [17,18].

The C_{10} value reached with the graphitized CFs FT 700 and UCC-22 of about 300 mAh/g is higher than that reported by Iijima et al. [7]. This remark applies also for the T 300 PAN-based CF as we obtained a reversible capacity of 175 mAh/g, when Imanishi et al. [3] found only 50 mAh/g. This could be attributed to a better choice of CFs/AB/PEO/PE weight ratio in the

Table 2
Electrochemical characteristics of the tested carbon materials during the first and the tenth charge/discharge cycles: e_0 = cell initial OCV, D_1, C_1 = discharge, charge capacity, η_{F1} = faradaic yield = C_1/D_1

Type of carbon fibre	e_0 (mV)	D_1 (mAh/g)	C_1 (mAh/g)	η_{F1} (%)	D_{10} (mAh/g)	C_{10} (mAh/g)	η_{F10} (%)
FT 700	1420	365	305	83	327	301	92
UCC-32	1350	357	309	86	327	297	91
UCC-2	1540	353	296	81	297	279	94
FT 500	1640	305	253	82	261	246	94
T 300	1480	260	197	75	189	175	93

composite electrode which may allow better electron and ion homogenization.

3.2.2. Polymer electrolyte

Fig. 3 shows the two first galvanostatic charge/discharge cycles under a $C/20$ regime (LiC_6 reached in 20 h). The first discharge branch takes more than 45 h compared with the 15 h of the first charge branch. The faradaic yield is therefore about 1/3. The second cycle has a yield close to 1, the amount of reversible stored/released electricity corresponds to $15/20 = 0.75$ F/C_6. Assuming that some amount δ of lithium is irreversibly intercalated during the first discharge and forms a residual compound $Li_\delta C_6$ [17], the electrode reaction should be written as follows:

$$Li_\delta C_6 + 0.75Li^+ + 0.75e^- \underset{\text{discharge}}{\overset{\text{charge}}{\rightleftharpoons}} Li_{\delta+0.75}C_6 \qquad (2)$$

therefore, δ should be lower than 0.25 considering that in natural graphite, LiC_6 is the richest phase attained in the experiment conditions.

Using a chemical analysis technique, Guérard [17] showed that the lithium remaining after de-intercalation corresponds to an average δ close to 0.1 and Bittihn et al. [18] found δ close to 0.25 by electrochemical measurement in agreement with our results under the reasonable assumption that LiC_6 is formed at the end of each discharge. As a matter of fact, we have observed a homogeneous golden colour of the graphite flakes after full lithium intercalation characteristic of stage-1 LiC_6.

The reversible stage formation should bear a relation to the successive potential plateaus as magnified in inserts A, B, C for the charge/discharge curves in Fig. 3. These plateaus are similar to those previously obtained

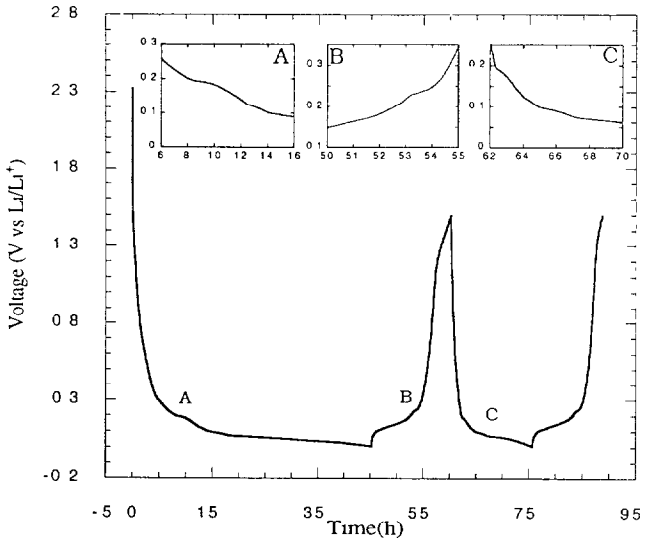

Fig 3. First and second galvanostatic ($C/20$) discharge/charge cycles of the Li/P(EO)$_8$LiClO$_4$/natural graphite-based Li$_x$C$_6$ electrode at 80 °C Inserts A, B and C give more details of the curves

in the highly oriented pyrolytic graphite sample [19,20], and attributed to staging, ideally schemed by:

$$\underset{\text{stage}\geqslant 3}{LiC_{24}} \rightleftharpoons \underset{\text{stage-2}}{LiC_{18}/LiC_{12}} \rightleftharpoons \underset{\text{stage-1}}{LiC_6} \qquad (3)$$

It is worth noticing that the faradaic yield of the first cycle is lower in the P(EO)$_8$LiClO$_4$ electrolyte than the one commonly observed in liquid media in the same potential window [14,15]. The differences in the apparent stability at low potential (about 0 V versus Li^+/Li) between PEO on one hand and EC/PC on the other hand may explain the lower faradaic yield of the PEO. In the liquid solution the formation of the passivating layer at the carbon surface occurs mainly during the first step of the electrode reduction which then allows only unsolvated lithium to be intercalated, whereas in PEO medium the intercalation should occur before the electrolyte cathodic decomposition. The possibility is not excluded that the highly oxidizing ClO_4^- anion present in the polymer electrolyte may be reduced on the graphite surface and so contribute to the irreversible behaviour during the first cycle.

A recent study on the lithium/PEO interface showed that, similarly to the case in a liquid electrolyte, a passivating layer is formed on the lithium surface in contact with PEO [21]. Since at low potential, a competition between the lithium plating and intercalation into graphite takes place [19], a passivating layer should be formed as long as metallic lithium is present on the graphite surface. In addition, the lithium chemical diffusion rate into graphite decreases with increasing lithium concentration at the graphene edges, leading to a higher irreversible consumption of the metal and therefore to a lower faradaic yield.

When the passivating layer is formed, the faradaic yield tends to unity and the actual reversible capacity reaches around 280 mAh/g in accordance with Eq. (2). This indicates the good chemical and dimensional stability of the passivated graphite/PEO interface.

3.3. Voltammetry and thermodynamic measurements

The lithium extraction from stage-1 LiC_6 prepared by the chemical lithiation of natural graphite at 400 °C using the vapour phase technique [22] was carried out in a similar Li/P(EO)$_8$LiClO$_4$/LiC_6 cell by voltammetric technique at a 1 mV/min sweep rate at 80 °C. Fig. 4 shows one oxidation peak at 95 mV versus Li^+/Li which should be associated to the stage-1 → stage-2 transition.

A similar Li/P(EO)$_8$LiClO$_4$/LiC_6 cell was used in order to establish the temperature dependence of the open-circuit voltage (OCV). Measurements were carried out between 76 and 117 °C and reported in Fig. 5 which shows a good linear behaviour. The $OCV = f(T)$ follows the approximate law: $e(mV) = 110.2 - 0.0512\ T$

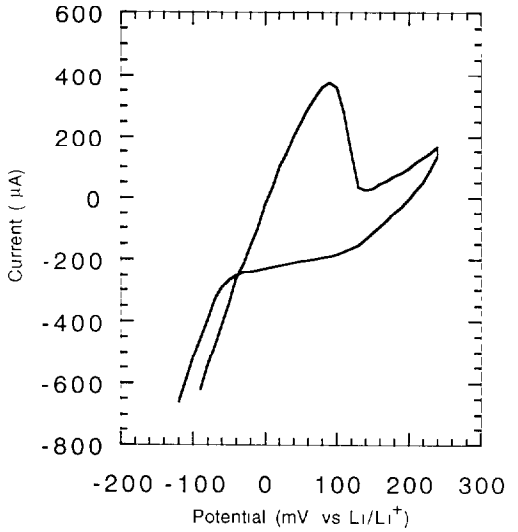

Fig 4. Lithium extraction from chemically prepared LiC_6 from natural graphite in Li/polymer electrolyte cell at 80 °C; voltage sweep scan = 1 mV/min

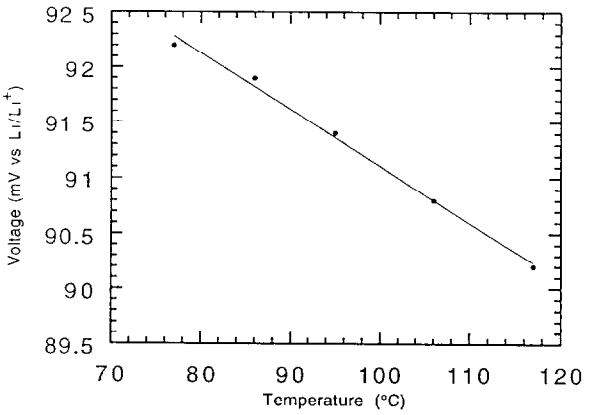

Fig. 5 Temperature dependence of the open-circuit voltage of a $Li/P(EO)_8LiClO_4/LiC_6$ cell

(T in K). Using the classical thermodynamics equations:

$$\Delta S = F\frac{\partial e}{\partial T},\ \Delta G = -eF \text{ and } \Delta H = F\left(T\frac{\partial e}{\partial T} - e\right) \quad (4)$$

where ΔS, ΔG and ΔH are respectively the cell reaction entropy, free energy and enthalpy; one obtains: $\Delta S = -4.94$ J/Li mol/K; $\Delta G = -8.9$ kJ/Li mol at 80 °C, and $\Delta H = -10.63$ kJ/Li mol. These values are lower than those reported in the highly oriented pyrolytic graphite samples [19], probably due to the better homogeneity of the chemically prepared powder sample.

4. Conclusions

The reversibility of the lithium insertion in different carbon materials was studied in liquid and solid state electrolytes. For the MCFs in the liquid medium, the reversible capacity increases with the degree of graphitization to reach about 300 mAh/g for the FT 700 and UCC-32 fibres. The low faradaic yield of the first cycle can result from the formation of a passivation film, but probably also from a less efficient wetting of carbon by the solid electrolyte and from the occurrence of residual lithium in the carbon host lattice.

In the polymer electrolyte, a reversible capacity as high as 280 mAh/g was achieved which makes it possible to use LiC_6 as a negative electrode in polymer-type rocking-chair lithium batteries.

References

[1] T. Nagaura and K Tozawa, *Prog Batteries Solar Cells, 9* (1990) 209.
[2] K Ozawa and M Yokokawa, *Proc 10th Int Seminar Primary and Secondary Battery Technology and Applications, March 1–4, 1993, Deerfield Beach, FL, USA*
[3] N. Imanishi, S Ohashi, T Ichikawa, Y Takeda, O Yamamoto and R Kanno, *J Power Sources, 39* (1992) 185
[4] R. Kanno, Y Kawamoto, Y Takeda, S Ohashi, N. Imanishi and O. Yamamoto, *J Electrochem Soc., 139* (1992) 3397.
[5] N Imanishi, H. Kashiwagi, T Ichikawa, Y. Takeda, O Yamamoto and M. Inagaki, *J. Electrochem Soc., 140* (1993) 315
[6] M. Endo, J. Nakamura and A Emori, *Proc 21 Biennial Carbon Conf, 1993, Essen, Germany*, p. 608; M Endo, J. Nakamura, A Emori and Y. Sasabe, *Mol Cryst Liq. Cryst, 245* (1994) 171.
[7] T. Iijima, K. Susuki and M Sato, *31st Jap Batt Symp, Osaka, Japan, 1990,* p 273
[8] M. Ide, M Mizutani and M. Yamachi, *32st Jap Batt Symp, Kyoto, Japan, 1991,* p 147.
[9] M. Morita, N. Nishimura, H. Tsutsumi and Y. Matsuda, *Chem. Express, 6* (1991) 619
[10] C.K. Huang, S. Surampudi, A. Attia and G Halpert, in S Surampudi and V.R Koch (eds.), *Proc Symp. Lithium Batteries,* The Electrochemical Society, Vol 93–4, p. 32
[11] K Sekai, H. Azuma, A. Omaru, S. Fujita, H. Imoto, T Endo, K. Yamaura and Y. Nishi, *J. Power Sources, 43* (1993) 241.
[12] R Yazami, Ph Touzain and L Bonnetain, *Synth Met, 7* (1983) 169.
[13] O Chusid, Y. Ein Ely, D Ubach, M. Babai and Y Carmelli, *J Power Sources, 43* (1993) 47.
[14] R Fong, V. Von Saken and J.R Dahn, *J Electrochem Soc, 137* (1990) 2009
[15] P. Scholerbock and M H Boehm, *Mater Sci Forum, 91–93* (1992) 683
[16] R Yazami, in G Pistoia (ed), *Lithium Batteries, New Materials, Developments and Perspectives,* Elsevier, 1994, p 49.
[17] D. Guérard, *Ph D Thesis,* University of Nancy, France, 1974
[18] R Bittihn, R. Herr, D Hoge and D. Ilic, *J Power Sources, 43* (1993) 223.
[19] R Yazami and Ph. Touzain, *J Power Sources, 9* (1983) 365.
[20] D. Billaud, F.X Henry and P Willmann, *Mol. Cryst Liq Cryst, 245* (1994) 159.
[21] F. Croce and B Scrosati, *J Power Sources, 43* (1993) 9.
[22] D Guérard and A. Hérold, *Carbon, 13* (1975) 337